

Proposal of Aerospace-informatics by Design of Ramjet Inlet Using Machine Learning

Seungho Lee*, Sunho Lee**, Jaehyuk Huh**, and Sejin Kwon[†]

*Department of Aerospace Engineering, Korea Advanced Institute of Science and Technology (KAIST)
291, Daehak-ro, Yuseong-gu, Daejeon, 34141, Republic of Korea

**School of Computing, Korea Advanced Institute of Science and Technology (KAIST)
291, Daehak-ro, Yuseong-gu, Daejeon, 34141, Republic of Korea

myshlee520@kaist.ac.kr · myshlee417@casys.kaist.ac.kr · jhhuh@casys.kaist.ac.kr · trumpet@kaist.ac.kr

[†]Corresponding author

Abstract

In this research, aerospace-informatics was proposed by design of ramjet inlet using machine learning. The model was organized in three steps. First, the maximum combustion chamber pressure and air mass flow rate error according to the shape was predicted. Second, the shape was discriminated whether it is feasible or not. Third, the shape with the high maximum combustion chamber pressure, the low air mass flow rate error, and the high feasibility was recommended. As a result, our proposed mechanism correctly predicted the pressure and the mass flow rate error, and sorted the ramjet design except crossing two less-important designs.

1. Introduction

Aerospace engineering has rapidly grown thanks to trends of private sector led space development and independent national defense, and has continuously produced enormous unprocessed data. Studies to process aerospace data will be needed inevitably. Informatics of computer science has been widely applied to various fields of industry, academia, and research. Bio-informatics was introduced to extract meaningful results from vast unrefined biological data. Therefore, aerospace-informatics as interdisciplinary research between aerospace engineering and computer science was suggested with the example of design of ramjet inlet using machine learning.

Ramjet is a class of air-breathing jet in supersonic speed and utilizes momentum to make air with high pressure and high temperature for combustion and propulsion.²⁰ Artillery is one of methods to initially accelerate projectile such as artillery shell to supersonic speed. For example, 410 mm gun of HARP (High Altitude Research Project) was developed to send projectile to 180 km.¹⁸ Thus, gun launched solid fuel ramjet propulsion system is reasonable to extend range of artillery shell. For example, 155 mm HE-ExR of Nammo is being developed for extreme range.¹¹ According to Nammo, ranges of artillery shells with BB (Base Bleed) or RAP (Rocket Assisted Projectile) are 40 km and 85 km respectively, but that with SFRJ (Solid Fuel RamJet) is 100 km or more.¹¹ A number of studies about each component such as concept, inlet, combustion chamber, and nozzle have been investigated theoretically and experimentally.^{3,6-9,12,16,17,23} However, those about design procedure to combine them are scarcely published because gun launched solid fuel ramjet artillery shell is state-of-the-art and classified technology.

In this research, with the instance of gun launched solid fuel ramjet propulsion system at muzzle of Poongsan in development, design of ramjet inlet using machine learning was conducted to propose aerospace-informatics.

2. Variables of Ramjet Inlet

Figure 1 shows schematic of gun launched solid fuel ramjet propulsion system. Gun launched solid fuel ramjet propulsion system consisted of inlet, combustion chamber, and nozzle. Inlet consisted of supersonic diffuser, diffuser throat, and subsonic diffuser. Furthermore, supports consisted of inlet support, diffuser throat support, subsonic diffuser support, combustion chamber and nozzle support, and artillery shell support. Explosive was mostly contained in inlet. Design point was initial condition instantly after gun launch at muzzle, and all parameters were feedback to one another.

RFP (Request For Proposal) was demanded by Poongsan. Table 1 shows specifications of RFP. Range was determined to achieve minimum objective. Artillery shell mass and artillery shell length were determined to maximize explosive

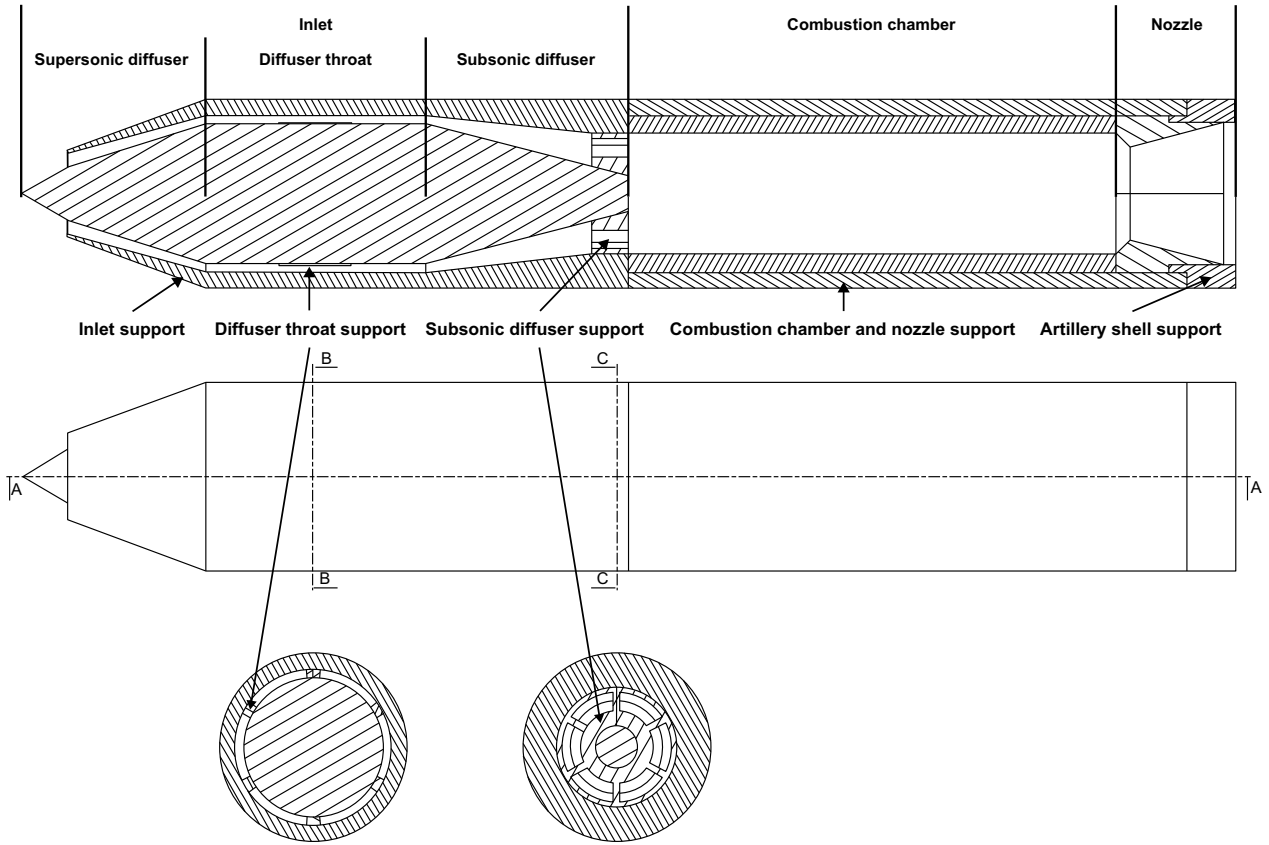


Figure 1: Schematic of gun launched solid fuel ramjet propulsion system.

Parameter	Value	
	Demanded	Determined
Range	$\geq 100 \text{ km}$	$\sim 100 \text{ km}$
Artillery shell mass	$\leq 50 \text{ kg}$	50 kg
Artillery shell length	$\leq 1000 \text{ mm}$	1000 mm
Artillery shell diameter		155 mm
Artillery shell velocity, Muzzle velocity		900 m/s

Table 1: Specifications of RFP.

quantity. Artillery shell diameter and artillery shell velocity, also known as muzzle velocity, were determined in consideration of existing artillery shell of Poongsan.

Figure 2 shows schematic of inlet. Table 2 shows specifications of inlet. Because of 14 parameters, the number of shapes is massive, so it is necessary to define constraint with controlled variable, and inevitable to conduct iteration with manipulated variable.

Controlled variable was established as follows. Artillery shell radius was determined as half of artillery shell diameter. Inlet length was determined as half of artillery shell length and compromise between explosive quantity and combustion chamber and nozzle length. Inlet support thickness was determined as compromise between explosive quantity and structural analysis. Subsonic diffuser exit width, subsonic diffuser support internal radius, and subsonic diffuser support length were determined in consideration of existing artillery shell of Poongsan. In Eq. 1, capture area radius was calculated from air mass flow rate. Atmospheric density was determined from references.¹

$$r_{ca} = \sqrt{\dot{m}_a / (\pi v \rho)} \quad (1)$$

In Eq. 2, air mass flow rate was calculated from thrust, specific impulse, and fuel air ratio. Gravitational acceleration was determined from references.¹

$$\dot{m}_a = \dot{m}_f / FAR = F_T / (I_{sp} g FAR) \quad (2)$$

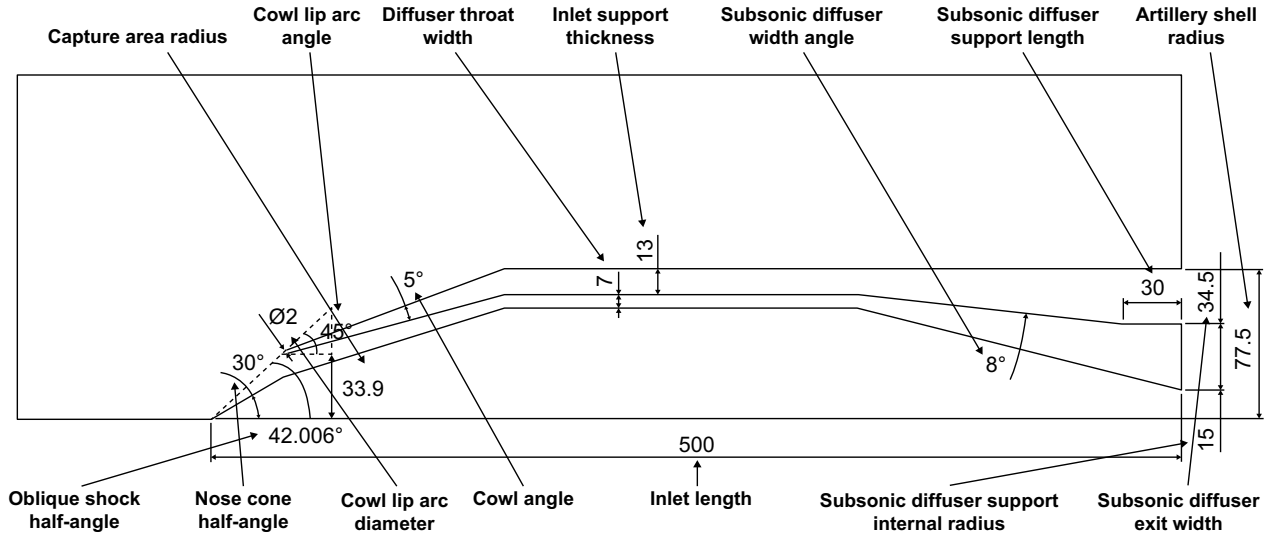


Figure 2: Schematic of inlet.

Controlled variable	Value	Unit
Artillery shell radius	77.5	mm
Inlet length	500	mm
Inlet support thickness	13	mm
Subsonic diffuser exit width	34.5	mm
Subsonic diffuser support internal radius	15	mm
Subsonic diffuser support length	30	mm
Capture area radius	33.9	mm
Nose cone half-angle	30	°
Oblique shock half-angle	42.006	°

Manipulated variable	Minimum value	Maximum value	Interval	Determined value	Unit
Cowl lip arc diameter	1	5	1	2	mm
Cowl lip arc angle	0	90	15	45	°
Cowl angle	3	8	1	5	°
Diffuser throat width	6	13	1	7	mm
Subsonic diffuser width angle	5	11	1	8	°

Table 2: Specifications of inlet.

Thrust was determined from drag and thrust-equal-drag condition with margin.³ In Eq. 3, drag was calculated. Elevation angle was determined to maximize range. Drag coefficient was determined in consideration of existing artillery shell of Poongsan.

$$F_D = mg \sin \theta + 0.5 \rho_a v^2 C_d (\pi D^2 / 4) \quad (3)$$

In Eq. 4, specific impulse was calculated from fuel air ratio and rocket specific impulse, and they were computed by NASA CEA (Chemical Equilibrium with Applications) with problem type of rocket, reactant fuel-oxidant mixture of equivalence ratio in terms of fuel oxidant ratio, combustion chamber of infinite area and equilibrium, and exit condition of sea level.^{4,5,14} Combustion chamber pressure was determined as estimate that can be modified according to results of after-mentioned Ansys Fluent. Atmospheric pressure was determined from references.¹ Fuel composition was determined from references.^{8,9} HTPB chemical formula and HTPB enthalpy of formation were determined from references.¹⁹ Propellant temperature was determined as estimate of inlet exit temperature that can be modified according to results of after-mentioned Ansys Fluent. Rocket specific impulse according to fuel air equivalence ratio, fuel air ratio, and combustion chamber pressure was computed. Fuel air equivalence ratio was divided between 0.9 and 1.1 at interval of 0.05. Combustion chamber pressure was divided between 10 bar and 13 bar at interval of 0.5 bar. Fuel air equivalence ratio and fuel air ratio were determined to maximize rocket specific impulse. Moreover, specific impulse efficiency based on typical ramjet specific impulse was determined from references.²

$$I_{sp} = F_T / (\dot{m}_f g) = (\dot{m}_f + \dot{m}_a) I_{sp,rocket} g / (\dot{m}_f g) = (1 + 1/FAR) I_{sp,rocket} \quad (4)$$

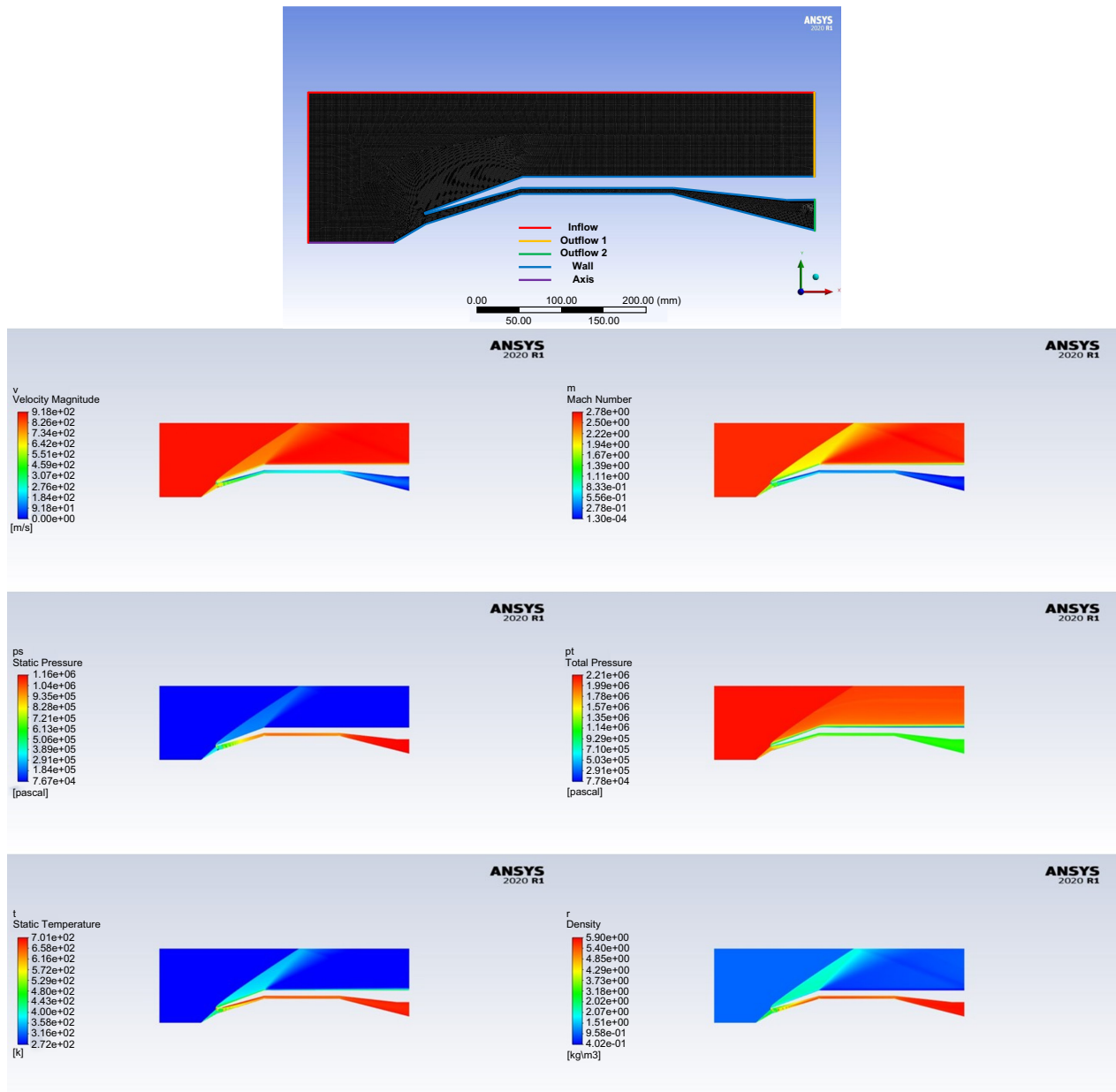


Figure 3: Schematic of results of mesh, velocity, Mach number, pressure, total pressure, temperature, and density.

Parameter	Value
Inlet exit velocity	105.6846 <i>m/s</i>
Inlet exit Mach number	0.2016
Inlet exit total pressure	11.8472 <i>bar</i>
Inlet exit temperature	684.5001 <i>K</i>
Inlet exit density	5.8513 <i>kg/m³</i>
Air mass flow rate	3.9429 <i>kg/s</i>
Inlet total pressure recovery	0.5424
Inlet exit temperature error	1.6861%
Air mass flow rate error	0.5875%

Table 3: Results of Ansys Fluent.

Parameter	Value
Atmospheric density	1.2250 <i>kg/m³</i>
Gravitational acceleration	9.8066 <i>m/s²</i>
Elevation angle	45 °
Drag coefficient	0.35
Drag	3623.2327 <i>N</i>
Thrust	3800 <i>N</i>
Combustion chamber pressure	11.5 <i>bar</i>
Atmospheric pressure	1.01325 <i>bar</i> , 1 <i>atm</i>
Combustion chamber pressure to atmospheric pressure ratio	11.3496
Fuel composition	80 <i>wt.%</i> HTPB, 15 <i>wt.%</i> AP, 5 <i>wt.%</i> Al
HTPB chemical formula	$C_{7.1102}H_{10.813}O_{0.1375}N_{0.1071}$
HTPB enthalpy of formation	-31.57 <i>kJ/mol</i>
Propellant temperature	673.150 <i>K</i> , 400 °C
Fuel air equivalence ratio	1.05
Fuel air ratio	0.0977
Rocket specific impulse	1728.2 <i>m/s</i> , 176.2283 <i>sec</i>
Specific impulse efficiency	0.5051
Specific impulse	1000 <i>sec</i>
Fuel mass flow rate	0.3875 <i>kg/s</i>
Air mass flow rate	3.9662 <i>kg/s</i>
Air specific heat ratio	1.400
Universal gas constant	8.31447 <i>kJ/kmolK</i>
Air molar mass	28.97 <i>kg/kmol</i>
Atmospheric temperature	288.150 <i>K</i> , 15.000 °C
Air specific gas constant	0.2870 <i>kJ/kgK</i>
Atmospheric speed of sound	340.2643 <i>m/s</i>
Artillery shell Mach number	2.65
Oblique shock quantity	1
Cowl lip type	Arc
Inlet entrance total pressure	21.8426 <i>bar</i>

Table 4: Specifications of gun launched solid fuel ramjet propulsion system.

Nose cone half angle was computed by NASA Supersonic Cone Simulator from artillery shell Mach number and oblique shock half angle for maximum supersonic diffuser total pressure recovery.^{15,21,22} In Eq. 5, artillery shell Mach number was calculated. Air specific heat ratio, universal gas constant, and air molar mass were determined from references.¹⁰ Atmospheric temperature was determined from references.¹

$$M = v/a = v/\sqrt{k_a R_a T} = v/\sqrt{k_a (R_u/M_a)T} \quad (5)$$

Oblique shock quantity was determined to simplify fabrication. Nose cone half angle according to artillery shell Mach number and oblique shock half angle for maximum supersonic diffuser total pressure recovery was arranged.^{16,17} Oblique shock half angle was computed by above-mentioned NASA Supersonic Cone Simulator.^{15,21,22}

Manipulated variable was established by as follows. Ramjet modes of operation are classified into ideal critical mode, subcritical mode with air mass flow rate loss, and supercritical mode with total pressure recovery loss.⁶ Maximum combustion chamber pressure with ramjet mode of operation of critical mode or supercritical mode closest to critical mode according to manipulated variable was computed by Ansys Fluent with axisymmetric 2D space solver, double precision option, density-based type solver, Navier-Stokes equation, implicit formulation, and SST k-omega viscous model. If maximum combustion chamber pressure was higher than before-mentioned estimate of combustion chamber pressure, design procedure with modified combustion chamber pressure was conducted again. Cowl lip type was

Terminology	Expression	Brief Description
Ramjet Design (R)	$R \leftarrow \begin{pmatrix} Feature(1) \\ Feature(2) \\ \vdots \\ Feature(n) \end{pmatrix}$	R is the vector of several features. We consider 5 features.
Pressure (P_R)	$P_R \leftarrow \operatorname{argmax}_P(Util(R, P))$	P_R is the max-utilized pressure (critical ramjet mode).
Mass Flow Rate Error ($MFRE_R$)	$MFRE_R \leftarrow Error(MFR_R, MFR_{std})$	$MFRE_R$ is the error from the standard MFR (MFR_{std}).
Feasibility ($Feasibility_R$)	$Feasibility_R = Prob_{SVM}[feasible]$	$Feasibility_R$ is the SVM probability of feasible class.
Objective Function ($O(R)$)	$O(R) = (pP_R) / (qMFRE_R) \times (rFeasibility_R)$	$O(R)$ is the weighted value of $P_R, MFRE_R, Feasibility_R$.

Table 5: Terminology and Expression of Ramjet Design.

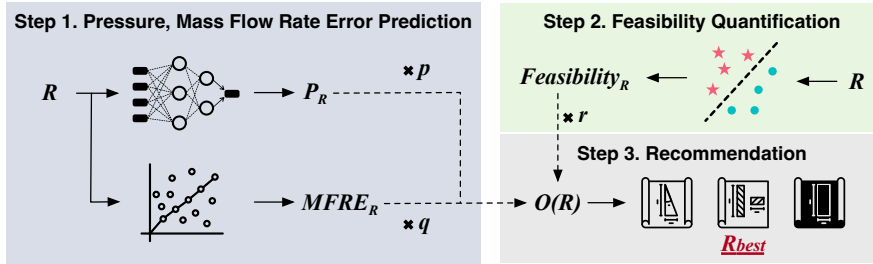


Figure 4: The Overview of The Ramjet Design Recommendation.

determined to simplify fabrication. Cowl lip arc diameter and diffuser throat width were divided at interval of 1 mm. Cowl lip arc angle was divided at interval of 15°. Cowl angle and subsonic diffuser width angle were divided at interval of 1°. Combustion chamber pressure was divided at interval of 0.5 bar. Cowl lip arc diameter, cowl lip arc angle, cowl angle, diffuser throat width, and subsonic diffuser width angle were determined as designable value and compromise between explosive quantity and structural analysis. Figure 3 shows schematic of results of mesh, velocity, Mach number, pressure, total pressure, temperature, and density. Table 3 shows results of Ansys Fluent. Inlet exit velocity, inlet exit Mach number, inlet exit total pressure, inlet exit temperature, and inlet exit density were computed as mass-weighted average. In order to evaluate performance, inlet total pressure recovery, inlet exit temperature error, and air mass flow rate error were calculated. Inlet total pressure recovery was calculated from inlet entrance total pressure. In Eq. 6, inlet entrance total pressure was calculated.

$$P_t = P(1 + (k_a - 1)M^2/2)^{k_a/(k_a-1)} \tag{6}$$

Inlet total pressure recovery including total pressure recoveries of supersonic diffuser, diffuser throat, and subsonic diffuser was reasonable. Inlet exit temperature error and air mass flow rate error were negligible.

Table 4 shows specifications of gun launched solid fuel ramjet propulsion system. All specifications not in other tables were tabulated.

3. Recommendation of Ramjet Inlet

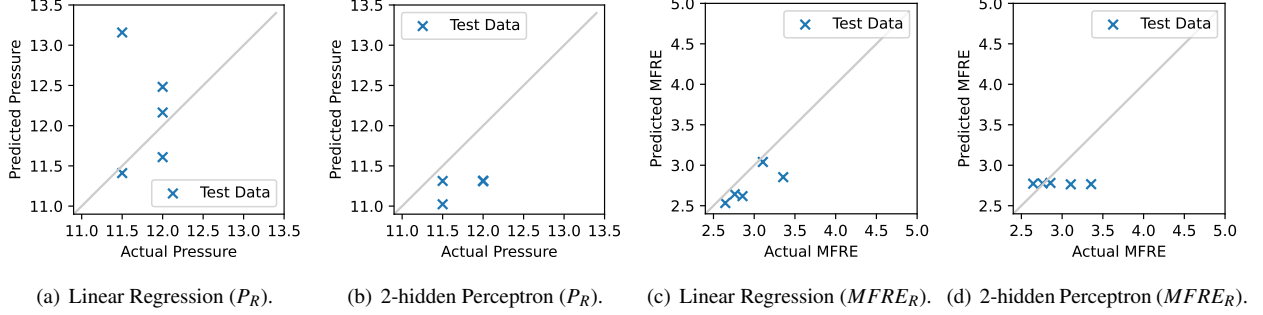
The ramjet design directly related to the performance and fuel efficiency. Therefore, the high-accurate technique of ramjet design selection is required within a reasonable latency. We suggest our 3-step machine learning method considering both predicted performance and the feasibility of the ramjet design. After the brief problem definition in Subsection 3.1, we introduce our solution in a high-level view in Subsection 3.2. From Subsection 3.3 to 3.5, we present the detailed evaluation methods and results.

3.1 Problem

Terminology and Expression: As shown as Table 5, we summarize several terminologies and expressions. The ramjet design (R) consists of several features. In this research, we leverage five features (the diameter of cowl lip arch, angle of cowl lip arc, cowl angle, diffuser throat width, and subsonic diffuser width angle) to form the ramjet design. Pressure (P_R), mass flow rate error ($MFRE_R$), and feasibility ($Feasibility_R$) are target variables. Since the

Model	Mean Squared Error (P_R)	Mean Squared Error ($MFRE_R$)
Linear Regression	0.6341	0.0681
2-hidden Perceptron Model	0.3709 (41.5% Improvement)	0.0952 (28.5% Degradation)

Table 6: Mean Squared Error of Pressure and Mass Flow Rate Error with Linear Regression and 2-Hidden Layer MLP.


 Figure 5: Actual and Predicted Test Value of P_R and $MFRE_R$.

critical ramjet operation mode shows the highest utilization among three mode (supercritical, critical, and subcritical), we define the pressure of the specific ramjet design (P_R) as a pressure in critical mode. According to the ramjet, the outlet mass flow rate is constant standard value (MFR_{std}). However, there are some error occur caused by the ramjet design. We define the error of mass flow rate ($MFRE_R$) as the error ratio compared to standard mass flow rate. There are many physical constraints of forming the ramjet design and the machine learning model. Feasibility ($Feasibility_R$) is the SVM possibility of the positive (feasible ramjet design) class. Therefore, the lower feasibility design means that it is un-realistic. The objective function consists of previous three values (P_R , $MFRE_R$, and $Feasibility_R$) to recommend the design considering both pressure, mass flow rate error, and feasibility.

Problem Description:

$$R_{best} = \operatorname{argmax}_{R_k} \left(\frac{pP_{R_k} \times rFeasibility_{R_k}}{qMFRE_{R_k}} \right) \quad (7)$$

when,

$$Feature(i) \leftarrow \begin{cases} User_Defined & (1 \leq i \leq m) \\ None_Defined & (otherwise) \end{cases} \text{ in } R_k, \quad Importance(P_R : MFRE_R : Feasibility_R) = p : q : r$$

The goal of the research is to find the feasible ramjet design (i.e the set of features) that makes highest pressure and lowest mass flow rate error. According to the environment, some features are strictly restricted and we consider these features as *User_Defined*. These *User_Defined* values are fixed in a single inference task and we try to find the best design by managing only *None_Defined*. Although we only consider m equals to the number of features and all features are *None_Defined* in this paper, we emphasize the model should not strictly limited by the single set of features. We remain this problem for our further works. According to the criteria of the good ramjet design, user sets the weighted values (p , q , and r). In this paper, we assigned the inverse of maximum distance of P_R , $MFRE_R$, and $Feasibility_R$ to each weight.

Evaluation Setup: We collect the data from Ansys Fluent simulation tool.¹³ Using the Intel Xeon E5-2660 (2.20GHz) Dual Core CPU, 80GB memory, and NVIDIA GeForce GTX 960 GPU machine, the analysis of a ramjet design with a pressure requires about 8 hours. We totally assemble 58 numbers of ramjet design as a dataset.

Challenge: The simulation of the ramjet design requires significant amount of time. In pressure computation, argmax operation needs to try many candidate pressure per each ramjet design. Moreover, the analysis of a single pressure consumes about 8 hours in our evaluation setup. Therefore, the prior recommendation limited to subset detection based on the empirical setting of users. To reduce and improve this time-consuming tasks, we propose the rapid recommendation mechanism using machine learning prediction models.

3.2 Overview

Figure 4 presents the overview of our ramjet design search. In a first step, the predict the pressure of the ramjet design using several models. We utilize linear regression and multi-layer perceptron (MLP) as a training model. Since

	Predicted: <i>positive</i>	Predicted: <i>negative</i>
Actual: <i>positive</i>	True-positive (TP): 33.3%	False-negative (FN): 0%
Actual: <i>negative</i>	False-positive (FP): 16.7%	True-negative (TN): 50.0%

Table 7: Classification whether the specific ramjet design is feasible (*positive*) or not (*negative*).

Cowl Lip Arc Diameter	Cowl Lip Arc Angle	Cowl Angle	Diffuser Throat Width	Subsonic Diffuser Width Angle	Rank(Actual)	Rank(Predicted)
1	0	3	6	8	5th	4th
1	15	5	12	5	3rd	3rd
1	0	3	9	6	2nd	2nd
1	0	3	7	6	1st	1st
1	0	3	6	9	4th	5th

Table 8: Actual and Predicted Rank of Five Test Ramjet Designs.

the ramjet design is limited by the several physical conditions, we use the SVM-based classification for detecting the unfeasible design. Unlike the simple binary classification problem, we focus on the case the classification sometimes misses the high-pressure design. To solve this drawbacks, we adopt the SVM probability of positive class as a feasibility value and simultaneously consider with the pressure. Based on our dataset, we finally suggest the objective function combined with weighted value (p, q, r in Figure 4) of pressure, mass flow rate error, and feasibility to quickly recommend the design among candidates.

3.3 Step 1. Pressure and Mass Flow Rate Error Prediction

We construct two linear models and multi-level perceptron (MLP) models with two hidden layers as a prediction model. Each linear model and each MLP model are trained for P_R , and $MFRE_R$ values. The 80% of data is assigned for training and the remained for test and set the training epochs as 60,000. The 2-hidden perceptron model has 4, 2 nodes in each hidden layer and every layer uses the sigmoid activation function.

As shown in Table 6, MLP model gets 41.5% improved mean squared error for P_R while it makes 28.5% degradation for $MFRE_R$ compared to the linear regression. Figure 5 shows the predicted and actual pressure of test data. Since the ideal predictor presents same predicted and actual value, the distance between $y = x$ line and the data point is important. Since the predicted values from our 2-hidden perceptron model are located in close to $y = x$ line in P_R cases, linear model shows better performance in $MFRE_R$ prediction. Therefore, we decide to choose the 2-hidden MLP model for P_R and linear model for $MFRE_R$ prediction.

3.4 Step 2. Feasibility of Ramjet Design

As the ramjet design is restricted by the physical constraints, we should consider the design is practicable. We utilize the SVM (Support Vector Machine) to classify the design into feasible (*positive*) and none-feasible (*negative*). Table 7 shows the correlation between actual value and predicted value. About 83.3% of test data (33.3% for True-positive + 50.0% for True-negative) is successfully classified. Although there are 16.7% of test data makes wrong prediction, there is no remained False-negative data which reduces the possibility of skipping the high-feasible data. Based on the SVM results, we decide the SVM probability of positive class for $Feasibility_R$ to the ramjet design search. It is generated by the `predict_proba` function in Scikit-Learn SVM library.

3.5 Step 3. Ramjet Design Recommendation

Ramjet design recommendation should consider not only pressure but also mass flow rate error and feasibility. Since they have different unit and degree, we define the object function as the weighted value of pressure, mass flow rate and feasibility to reflect the ratio of each value.

$$(p, q, r) = \left(\frac{1}{MAX(P_R) - MIN(P_R)}, \frac{1}{MAX(MFRE_R) - MIN(MFRE_R)}, \frac{1}{MAX(Feasibility_R) - MIN(Feasibility_R)} \right)$$

We set weights as the inverse of difference between maximum and minimum values. It corrects the different gap between other variables. Table 8 shows the five test data and their actual and predicted rank order. Since only the order

of 4th and 5th is different, our technique correctly results until the request of 1st to 3rd ramjet design in our example. (i.e until the highest 60% recommendation request)

4. Conclusions

Ramjet inlet was designed by using machine learning to suggest aerospace-informatics. Inlet variables included artillery shell radius, inlet length, inlet support thickness, subsonic diffuser exit width, subsonic diffuser support internal radius, subsonic diffuser support length, capture area radius, nose cone half angle, oblique shock half angle, cowl lip arc diameter, cowl lip arc angle, cowl angle, diffuser throat width, and subsonic diffuser width angle. In order to accomplish effective and efficient combustion, high combustion chamber pressure and low air mass flow rate error are generally required in critical mode without air mass flow rate loss in subcritical mode and combustion chamber pressure loss in supercritical mode. Iteration to investigate critical mode for every shape is immoderate, so machine learning was utilized for low cost of time. Three steps including pressure and mass flow rate error prediction, feasibility of ramjet design, and ramjet design recommendation was conducted. In summary, our prediction model selected the 2-hidden perceptron model for the pressure to get 41.5% improvement while adopted the linear model for the mass flow rate error to take 28.5% enhancement. Also, the feasibility mechanism successfully classified 83.3% amount of test data. Finally, our method made the accurate sorted list for the highest 60% designs with only trivial crossing error for minor 40% designs.

5. Acknowledgements

This research was supported by Poongsan-KAIST Future Technology Research Center funded by Poongsan.

Appendix A (Nomenclature)

a = Atmospheric speed of sound
 C_d = Drag coefficient
 D = Artillery shell diameter
 F_D = Drag
 F_T = Thrust
 FAR = Fuel air ratio
 g = Gravitational acceleration
 I_{sp} = Specific impulse
 $I_{sp,rocket}$ = Rocket specific impulse
 k_a = Air specific heat ratio
 M = Artillery shell Mach number
 M_a = Air molar mass
 m = Artillery shell mass
 \dot{m}_a = Air mass flow rate
 \dot{m}_f = Fuel mass flow rate
 P = Atmospheric pressure
 P_t = Inlet entrance total pressure
 R_a = Air specific gas constant
 R_u = Universal gas constant
 r_{ca} = Capture area radius
 T = Atmospheric temperature
 v = Artillery shell velocity, Muzzle velocity
 θ = Elevation angle
 ρ_a = Atmospheric density

References

- [1] US Standard Atmosphere. Nasa technical memorandum nasa-tm-x-74335, noaa-s/t-76-1562, 1976.
- [2] Eugene Fleeman. *Missile design and system engineering*. American Institute of Aeronautics and Astronautics, Inc., 2012.

- [3] Alon Gany. Analysis of gun-launched, solid fuel ramjet projectiles. *International Journal of Energetic Materials and Chemical Propulsion*, 1(1-6), 1991.
- [4] Sanford Gordon and Bonnie J McBride. Computer program for calculation of complex chemical equilibrium compositions and applications. part 1: Analysis. Technical report, 1994.
- [5] Sanford Gordon and Bonnie J McBride. Computer program for calculation of complex chemical equilibrium compositions and applications. part 2: users manual and program description. Technical report, 1996.
- [6] Joseph A Johnson III, Benjamin J Wu, YALE UNIV NEW HAVEN CT DEPT OF ENGINEERING, and APPLIED SCIENCE. Pressure recovery and related properties in supersonic diffusers: A review. *AFOSR Report*, (April), 59, 1974.
- [7] Woosuk Jung, Seungkwan Baek, Taesoo Kwon, Juhyeon Park, and Sejin Kwon. Demonstration of ethanol-blended hydrogen peroxide gas generator for ramjet combustor flow simulation. *Journal of Propulsion and Power*, 34(3):591–599, 2018.
- [8] Woosuk Jung, Seungkwan Baek, Juhyeon Park, and Sejin Kwon. Combustion characteristics of ramjet fuel grains with boron and aluminum additives. *Journal of Propulsion and Power*, 34(4):1070–1079, 2018.
- [9] Woosuk Jung, Sangwoo Jung, Taesoo Kwon, Juhyeon Park, and Sejin Kwon. Ignition delay in solid-fuel ramjet combustor. *Journal of Propulsion and Power*, 34(6):1519–1528, 2018.
- [10] Mehmet Kanoglu. *Thermodynamics: An engineering approach 8th edition in si units*. 2015.
- [11] THORSTEIN KORSVOLD. The range revolution (accessed 06 march 2023), 2019.
- [12] S Krishnan and Philmon George. Solid fuel ramjet combustor design. *Progress in aerospace sciences*, 34(3-4):219–256, 1998.
- [13] John E Matsson. *An Introduction to ANSYS Fluent 2022*. Sdc Publications, 2022.
- [14] NASA. Chemical equilibrium with applications (accessed 06 march 2023).
- [15] NASA. Supersonic cone flow interactive (accessed 06 march 2023).
- [16] Klaus Oswatitsch. Pressure recovery for missiles with reaction propulsion at high supersonic speeds (the efficiency of shock diffusers). In *Contributions to the Development of Gasdynamics: Selected Papers, Translated on the Occasion of K. Oswatitsch's 70th Birthday*, pages 290–323. Springer, 1980.
- [17] Klaus Oswatitsch and Ruedinger. *Contributions to the Development of Gasdynamics*. Springer, 1980.
- [18] Rely Victoria Petrescu, Raffaella Aversa, Bilal Akash, Filippo Berto, Antonio Apicella, and Florian Ion Petrescu. Project harp. *Journal of Aircraft and Spacecraft Technology*, 1(4):249–257, 2017.
- [19] Seongmin Rang, Junyeong Jeong, Vikas Khandu Bhosale, and Sejin Kwon. Reactivity of hypergolic hybrid solid fuel with industrial grade hydrogen peroxide. *Fuel*, 330:125543, 2022.
- [20] George P Sutton and Oscar Biblarz. *Rocket propulsion elements*. John Wiley & Sons, 2016.
- [21] Geoffrey Ingram Taylor and JW Maccoll. The air pressure on a cone moving at high speeds.âi. *Proceedings of the Royal Society of London. Series A, Containing Papers of a Mathematical and Physical Character*, 139(838):278–297, 1933.
- [22] Geoffrey Ingram Taylor and JW Maccoll. The air pressure on a cone moving at high speeds.âii. *Proceedings of the Royal Society of London. Series A, Containing Papers of a Mathematical and Physical Character*, 139(838):298–311, 1933.
- [23] Ronald G Veraar, Roelof Oosthuisen, and Kurt Andersson. Ramjet propulsion for projectiles- an overview of worldwide achievements and future opportunities. *International Journal of Energetic Materials and Chemical Propulsion*, 21(5), 2022.